International Conference on Nuclear Data for Science and Technology 2007
DOI: 10.1051/ndata:07488

Measurement of the ^{209}Bi(n,γ)^{210}Bi^{g} cross section and updated s-process analysis of the Pb/Bi region

S. Bisterzo[1,2,a], F. Käppeler[2], R. Gallino[1], M. Heil[4], C. Domingo-Pardo[2], C. Vockenhuber[5], and A. Wallner[6]

[1] Dipartimento di Fisica Generale, Università di Torino, via P. Giuria 1, 10125 (To), Italy
[2] Forschungszentrum Karlsruhe, Institut für Kernphysik, 76021 Karlsruhe, Germany
[3] Gesellschaft für Schwerionenforschung mbH (GSI), Planckstr. 1, 64291 Darmstadt, Germany
[4] TRIUMF, 4004 Wesbrook Mall, Vancouver, B.C., V6T 2A3 Canada
[5] Vienna Environmental Research Accelerator, Faculty of Physics, Universität Wien, Währinger Str. 17, 1090 Wien, Austria

Abstract. The neutron capture cross section of ^{209}Bi(n,γ)^{210}Bi has been measured using the 3.7 MV Van de Graaff accelerator at Forschungszentrum Karlsruhe. The measurement was carried out by activation of a high purity Bi sample in a quasi-stellar neutron spectrum with kT = 25 keV by employing the ^{7}Li(p,n)^{7}Be reaction at E$_p$ = 1912 keV. We performed four activations: two to count the α-activity of ^{210}Po and two more for Accelerator Mass Spectrometry (AMS) analysis at the VERA facility in Vienna. The aim of our study is to measure the partial cross sections to the ground and the isomeric state with improved accuracy, which is necessary to understand the recycling via α-decay of ^{210,211}Po and the corresponding accumulation of the s-process abundances at the end of the s-path. The Maxwellian averaged cross section for populating the ground state of ^{210}Bi at a thermal energy of kT = 30 keV was determined to be $\langle\sigma v\rangle/v_T$ = 2.16 ± 0.07 mb. For the isomeric state the measurements are in progress. Based on the present results and on the new data for the stable Pb isotopes measured at n_TOF, we performed a theoretical analysis using stellar models of Asymptotic Giant Branch (AGB) stars. The effect of the new cross section values in the Pb/Bi region was studied by averaging the results of stellar models for M = 1.5 and 3 M$_\odot$ and a half-solar metallicity for the main component, and at [Fe/H]= −1.3 for the strong component. At this lower metallicity the AGB stars have been shown to produce the maximum amount of s-process lead, thus providing a good approximation of the strong component. A study of these aspect is in preparation.

1 Introduction

^{209}Bi is the last stable isotope in the neutron capture chain of the s-process reaction path (fig. 1). Neutron capture on ^{209}Bi populates the isomer as well as the ground state of ^{210}Bi. At the higher s-process temperatures, when the ^{22}Ne(α,n) source is activated, the isomeric state ^{210}Bi^{m} is quickly depopulated to the short lived ground state by the photon bath and, therefore the neutron capture contributions are almost negligible. A more important role is played by the short-lived ground state ($t_{1/2}$ = 5.013 d), which β-decays into the α-unstable isotope ^{210}Po ($t_{1/2}$ = 138.38 d). Here starts the main recycling of the s-process via α-decay from ^{210,211}Po into ^{206,207}Pb. In light of this, improved nuclear physics data are necessary to estimate the accumulation of the s-process material beyond ^{206}Pb, and to consolidate the reliability of the Th and U chronometers. We present the result of the partial ^{209}Bi(n,γ)^{210}Bi cross section to the ground state by the measurement of the induced α-activity of ^{210}Po (see sect. 2), while the one to the isomeric state via Accelerator Mass Spectrometry (AMS) is in progress.

2 Measurement of ^{209}Bi(n,γ)^{210}Bi^{g} cross section

The neutron activation technique is well suited for determining the very small cross sections of isotopes with magic neutron numbers. The irradiations were carried out at the 3.7 MV Van de Graaff accelerator of Forschungszentrum Karlsruhe. Neutrons were produced via the ^{7}Li(p,n)^{7}Be reaction with a quasi-Maxwellian energy distribution of kT = 25.0 ± 0.5 keV [14]. The proton energy E_p = 1912 keV is adjusted slightly above the threshold of the reaction ($E_{p,th}$ = 1881 keV) to obtain a collimated neutron beam in a forward cone with an opening angle of 120° (fig. 2). A ^{6}Li glass neutron detector at 90 cm from the lithium target is used to monitor the flux in intervals of one minute. This information is needed for considering the decay and the fluctuations in the neutron yield during activation as described by the correction factor f_b. Two very thin Bi metal samples were prepared by evaporation to count the α-decay, and two more massive powder samples were pressed for the AMS measurement. The metallic bismuth

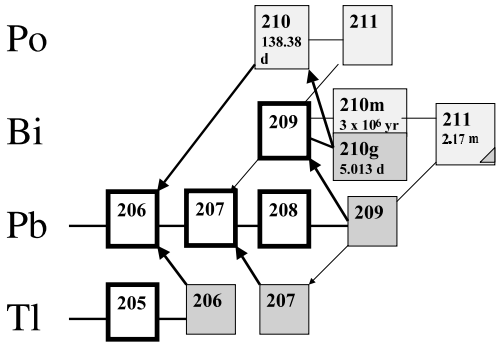

Fig. 1. The s-process path in the Pb/Bi region.

[a] Presenting author, e-mail: bisterzo@ph.unito.it

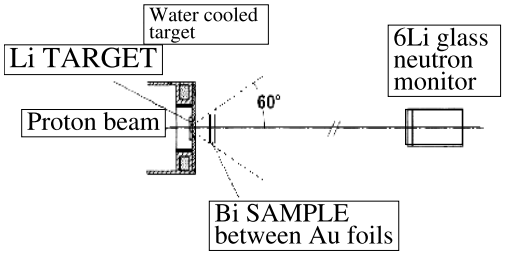

Fig. 2. Schematic setup of the activation measurement at the Van de Graaff accelerator.

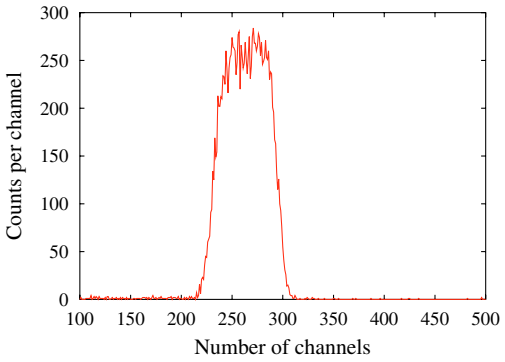

Fig. 3. The α-spectrum of the induced ^{210}Po activity in sample Bi3.

had a purity of better than 99.99%. The parameters used during the activation are summarized in table 1: m denotes the mass, d the diameter, x the thickness, N the number of atoms in the sample, t_a the activation time, and Φ the total time-integrated neutron flux. The related uncertainties listed in table 2 include the statistical and systematic errors as well.

Table 1. Activation parameters related to the investigated samples.

	Bi3	Bi6	BiA	BiB
m (mg)	2.98	2.32	214.96	233.36
d (cm)	1.00	1.00	0.60	0.60
x (μm)	3.9	3.0	281.	305
$N(10^{18}$ atoms)	8.59	6.69	619.43	672.45
t_a (d)	10.74	2.65	14.22	8.71
$\Phi(10^{14}$ n/cm^2)	7.27	1.99	6.29	13.02

Table 2. Uncertainties of the activation parameters (in %).

	Bi3	Bi6	BiA	BiB
m	0.01	0.01	<0.01	<0.01
d	0.10	0.10	0.17	0.17
x	1.03	1.32	0.93	0.93
N	0.94	1.21	0.01	0.01
t_a	0.01	0.05	0.01	0.02
Φ	1.82	3.26	0.98	1.15

During the irradiations the Bi samples were sandwiched between thin gold foils of the same diameter for normalization to the neutron capture cross section of gold at kT = 25 keV, which has been measured with great accuracy [14]. The main uncertainties concerning the evaluation of the averaged neutron flux result from the positioning of the sample between the two gold foils and relative to the target. Commonly, the induced γ-activity is counted after neutron irradiation. In the present case, the γ-lines related to the ground state decay of ^{210}Bi are very weak and are extremely difficult to detect via γ-spectroscopy with Ge-detectors. Therefore, very thin samples have been used in the first two activations for counting the α particles from the ^{210}Po decay with negligible absorption losses. Counting of the α-decay of ^{210}Po into ^{206}Pb (E_α = 5.304 MeV) started ≈20 days after the end of the activation

Table 3. Parameters of the α-measurement. Labels a and b denote two different α counting periods of the same sample.

	Bi3a	Bi3b	Bi6a	Bi6b
t_w (d)	20.16	43.32	88.28	115.09
t_c (d)	20.50	42.50	25.75	18.03
C_α	16313	14179	3368	2108
$\epsilon_\alpha(10^{-2})$	1.499	0.761	1.499	1.499
f_b	0.887	0.885	0.965	0.965

Table 4. Uncertainties of the parameters in table 3 (in %).

	Bi3a	Bi3b	Bi6a	Bi6b
t_w	0.02	0.01	<0.01	<0.01
t_c	0.02	0.01	0.01	0.02
C_α	0.18	0.21	4.45	1.42
ϵ_α	0.99	0.86	0.99	0.99

(corresponding to four half-lives of ^{210}Bi). The α-counting was performed with a Si-detector 23.72 ± 0.14 mm in diameter, which was mounted in a vacuum chamber several cm in front of the sample. The chamber was evacuated to 2×10^{-3} Pa with an oil-free pump. The α-spectrum of sample Bi3 is shown in figure 3 as an example.

The α measurement with the Si detector was carried out at two different distances from the sample Bi3 to evaluate the uncertainties of the detector efficiency. The various parameters and related uncertainties are listed in tables 3 and 4, respectively. The quantities listed are the waiting time between the irradiation and the beginning of α counting, t_w, the counting time, t_m, the number of counts, C_α, and the detection efficiency, ϵ_α. The latter quantity was determined by means of a GEANT-4 simulation and includes the uncertainties due to the counting geometry. The factor f_b is used to correct for the decay of ^{210}Po during the irradiation and for fluctuations in the neutron yield. This factor was evaluated by solving the differential equations of the number of atoms produced and decayed, from the start of the activation until the end of the α-counting with a MATHEMATICA simulation. The uncertainty of f_b turned out to be negligible since it depends only on the ^{210}Bi and ^{210}Po half-lives.

The experimental results for the (n,γ) cross section to the ground state of ^{210}Bi are summarized in table 5, yielding a weighted mean of

$$\langle\sigma_g\rangle(^{209}\mathrm{Bi}^g) = 2.23 \pm 0.07\ \mathrm{mbarn}.$$

Table 5. Experimental results for the partial (n,γ) cross section of ^{209}Bi to the ground state ^{210}Bi^{g}.

Samples	σ_{exp} [mbarn]	Total uncertainty [%]
Bi3a	2.279 ± 0.047	2.08
Bi3b	2.223 ± 0.045	2.03
Bi6a	2.197 ± 0.123	5.61
Bi6b	2.203 ± 0.081	3.69
weighted mean	2.23 ± 0.07	3.14

Table 6. Comparison with previous measurements of the partial and total (n,γ) cross sections at kT = 30 keV.

References	σ_{exp} [mbarn]
Ratzel et al. 2004 [15] (ground)	2.32 ± 0.14
This work (ground)	2.16 ± 0.07
Domingo-Pardo et al. 2006 [7] (total)	2.58 ± 0.50
Mutti et al. 1998 [13] (total)	2.54 ± 0.48
Beer et al. 1992 [2] (total)	3.12 ± 0.60

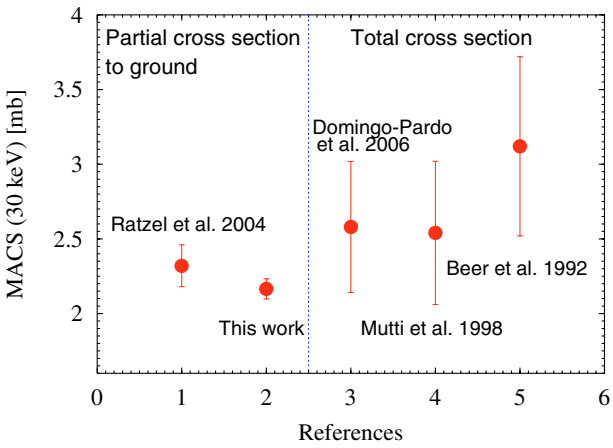

Fig. 4. Comparison with partial and total stellar (n,γ) cross sections for kT = 30 keV.

This value agrees within uncertainties with a previous measurement [15], which was carried out by detecting the electrons in the β-decay of ^{210}Bi^{g} (table 6). The agreement is even better if a new measurement of the α-half-life of ^{210}Po is considered. As reported in ref. [6], the present preliminary value is 142.0 ± 1.1 d instead of 138.376 ± 0.002 d given in [5]. The uncertainty of the new half life is still limited by the yet short measurement period of less than three half lives. Adopting this value the present experimental cross section becomes $\langle\sigma_g\rangle(^{209}\mathrm{Bi}^{g})$ = 2.27 ± 0.07 mbarn.

The Maxwellian averaged cross section (MACS) is obtained with a small correction for the cutoff in the experimental spectrum at 106 keV, yielding values of MACS(30 keV) $\langle\sigma_g\rangle$ = 2.16 ± 0.07 mbarn and 2.20 ± 0.07 mbarn for the decay rates of refs. [5,6], respectively.

The total (n,γ) cross section recently measured at n_TOF [7] is shown in table 6 together with previous results [2,13]. By averaging the total cross section values from refs. [7,13] we obtain an isomeric ratio, IR(30 keV)= $\sigma_m/\sigma_{\mathrm{tot}}$ = 0.15 ± 0.42, where $\sigma_m = \sigma_{\mathrm{tot}} - \sigma_g$. This value is too uncertain for comparison with the IR values at thermal energy (0.025 keV) reported in refs. [4,12,17]. As shown in figure 4, the measurements of the total (n,γ) cross section, which were carried out via the time-of-flight technique, are responsible for the large uncertainty in IR. Therefore it is important to apply the activation technique also for measuring the partial (n,γ) cross section to the isomer ^{210}Bi^{m}. While the long half-life of the isomer ($t_{1/2}$ = 3 × 10^6 yr) makes direct counting of the induced activity extremely difficult, the AMS technique provides an analytical method to detect with very high precision the produced ^{210}Bi nuclei through direct atom counting. This measurement is presently under way at the VERA facility in Vienna. First runs with this technique have shown that the necessary sensitivity for detecting the ^{210}Bi^{m} produced in the irradiations of samples BiA and BiB can indeed be reached. Figure 5 shows the signal obtained from the ground state decay of sample BiA compared to the background from non-irradiated material. We are planning to finish this analysis within 2007.

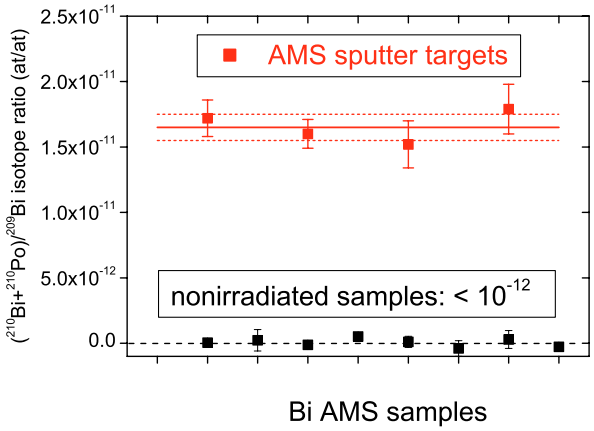

Fig. 5. Signal obtained in the AMS measurement of sample BiA compared to non-irradiated sample material.

3 Interpretation with stellar models

The main and strong s-process components are the site of the production of the s abundances from Sr up to Pb and Bi. The main s-process occurs in low mass, thermally pulsing AGB stars with about half of the solar metallicity, whereas the strong s-process takes place in low mass AGB stars of lower metallicity [11,16]. The major neutron source in these scenarios is the ^{13}C(α,n)^{16}O reaction, which burns radiatively at $T \approx 0.9 \times 10^8$ K during the interpulse period. A second weaker neutron source, the ^{22}Ne(α,n)^{25}Mg reaction, is partially activated during the convective thermal pulses, when the maximum temperature at the bottom of the He burning shell reaches values of $T \approx 3 \times 10^8$ K. The contribution from the main s-process to ^{209}Bi has been previously determined to 4.9% [1]. The metallicity dependence of the s-process was demonstrated by [11], who found that large amounts of ^{208}Pb and, consequently, a substantial increase of the ^{209}Bi abundance could be obtained at lower metallicities. The strong s-component in the solar system is the result of all previous generations of AGB stars in the Galaxy [18,19]. With the

Table 7. Abundance contributions from the main s-process (in %) compared to ref. [1].

	N_s (ref. [1])	N_s (this work)
^{204}Pb	94.3	91.7
^{206}Pb	57.8	65.9
^{207}Pb	63.7	57.5
^{208}Pb	34.5	41.3
^{209}Bi	4.9	5.5

Galactic Chemical Evolution (GCE) model used to compute the abundance trends versus metallicity of stars in a mass range from 1 to 8 $M_\odot$ in the three Galactic zones (thin disk, thick disk, and halo), it was shown that the strong and main component together produce 19% of solar ^{209}Bi.

According to the updated model described in [3] (average of the results for $M = 1.5$ and 3 $M_\odot$ and half-solar metallicity) with addition of the recent cross section values in the Pb/Bi region measured at n_TOF [7–10], the main s-process component provides 5.5% of the solar Bi. The main s-process contributions to the Pb isotopes and to ^{209}Bi are compared in table 7 with the previous results of ref. [1]. The sensitivity of these values with respect to variations of the Bi cross sections was shown in table VII of ref. [15]. We tested also the recycling of the s-process via α-decay of ^{210}Po, but this effect was found to be negligible. Moreover, since the isomeric state ^{210}Bi^m is likely depopulated to the short lived ground state at the higher temperatures of the relevant s-process scenarios, neutron captures to ^{211}Bi are negligible as well.

The average between the abundances obtained with 1.5 and 3 $M_\odot$ and with a metallicity [Fe/H]= -1.3, where AGB stars produce the maximum amount of s-process lead, represents a good approximation for the strong component. Compared to previous GCE computations, updated FRANEC models for stars of lower metallicity yield somewhat smaller s-process abundances. Consequently, the total s-process contribution (main plus strong) will also be smaller. Preliminary results indicate a contribution from the strong component of ≈35% for ^{208}Pb and ≈10% for ^{209}Bi, instead of 60% and 14% from the previous GCE model, respectively. This is an important result with respect to the r-process residuals, and hence for the interpretation of r-process abundance pattern of extremely metal-poor stars. A detailed study of these aspects is presently under preparation.

We would like to thank the Van de Graaff staff M. Brock, E.P. Knaetsch, and W. Seith for their support during the measurements.

References

1. C. Arlandini et al., ApJ **525**, 886 (1999).
2. H. Beer, F. Voss, R. Winters, ApJ Suppl. **80**, 403 (1992).
3. S. Bisterzo et al., *Proceedings of the International Symposium on Nuclear Astrophysics – Nuclei in the Cosmos - IX*, *25–30 June 2006*, CERN., p. 77.
4. A. Borella et al. (these proceedings).
5. S.Y.F. Chu, L.P. Ekström, R.B. Firestone, WWW Table of Radioactive Isotopes, database version, 28.2.1999, URL http//ie.lbl.gov/toi/index.htm.
6. R. Dressler et al., Annual Report, Paul Scherrer Institute, Villigen, Switzerland (2007).
7. C. Domingo-Pardo et al., Phys. Rev. C **74**, 025807 (2006).
8. C. Domingo-Pardo et al., Phys. Rev. C **74**, 055802 (2006).
9. C. Domingo-Pardo et al., Phys. Rev. C **75**, 015806 (2007).
10. C. Domingo-Pardo et al., Phys. Rev. C (2007) (in preparation).
11. R. Gallino et al., ApJ **497**, 388 (1998).
12. A. Letourneau et al., in *Proceedings of the 11th Int. Symp. on Capture Gamma Ray Spectroscopy and Related Topics*, edited by J. Kvasil, P. Cejnar, M. Kritcka (World Scientific, New Jersey, 2003), p. 734.
13. Mutti et al., *Nuclei in the Cosmos V*, edited by N. Prantzos, S. Harissopulos (Éditions Frontières, Paris, 1998), p. 204.
14. W. Ratynski, F. Käppeler, Phys. Rev. C **37**, 595 (1988).
15. U. Ratzel et al., Phys. Rev. C **70**, 065803 (2004).
16. O. Straniero et al., ApJ **478**, 332 (1997).
17. M. Takiue, H. Ishikawa, Nucl. Instrum. Meth. **148**, 157 (1978).
18. C. Travaglio et al., ApJ **549**, 346 (2001).
19. C. Travaglio et al., ApJ **601**, 864 (2004).